oy, 8

NOV 28 1973

A METHOD FOR THE PREDICTION OF
THE EFFECTS OF FREE-STREAM DISTURBANCES
ON BOUNDARY-LAYER TRANSITION

J. A. Benek and M. D. High

ARO, Inc.

October 1973

PROPULSION WIND TUNNEL FACILITY

ARNOLD ENGINEERING DEVELOPMENT CENTER

AIR FORCE SYSTEMS COMMAND

ARNOLD AIR FORCE STATION, TENNESSEE

NOTICES

A METHOD FOR THE PREDICTION OF
THE EFFECTS OF FREE-STREAM DISTURBANCES
ON BOUNDARY-LAYER TRANSITION

J. A. Benek and M. D. High
ARO, Inc.

.

FOREWORD

The research reported herein was conducted by the Arnold Engineering Development Center (AEDC), Air Force Systems Command (AFSC), under Program Elements 64719F and 65802F. Technical monitoring of the effort was performed by Captain Carlos Tirres, USAF, Research and Development Division, Directorate of Technology.

The results presented were obtained by ARO, Inc. (a subsidiary of Sverdrup & Parcel and Associates, Inc.), contract operator of AEDC, AFSC, Arnold Air Force Station, Tennessee. The study was conducted from January 1972 through March 1973 under ARO Project Nos. PW3101, PW5201, and PF206, and the manuscript was submitted for publication on June 27, 1973.

This technical report has been reviewed and is approved.

CARLOS TIRRES
Captain, USAF
Research and Development
    Division
Directorate of Technology

ROBERT O. DIETZ
Director of Technology

ABSTRACT

A semiempirical expression for boundary-layer transition location is developed based on the concept of a critical ratio of inertial to viscous shearing stresses at laminar breakdown. Extensive comparisons between predicted and measured transition locations on a 10-deg included-angle cone at transonic speeds are shown with the data predicted to within 10 percent. Comparisons are also made with low subsonic and supersonic data which indicate the method is extendible to these flow regimes.

CONTENTS

ILLUSTRATIONS

NOMENCLATURE

A   Value of $F'(\eta)$ at η_c

a_∞ Free-stream speed of sound, ft/sec

B   Value of $G'(\eta)$ at η_c

C   Constant of proportionality between boundary-layer thickness and Reynolds number

$F(y), G(y)$	Polynomial functions of y in Pohlhausen boundary-layer velocity profile
f	Compressibility correction factor
K_1	Constant defined in Section 3.1
K_2	Constant defined in Section 3.1
k	R_D/C
k_1	$k\sqrt{R_E X_t}$
L	Prandtl mixing length
ℓ	Characteristic length of transition model, 36 in.
M	Mach number
M_f	Fluctuating Mach number based on root-mean-square fluctuating velocity component
p	Pressure, psfa
$\bar{p}$	Steady-state (time-averaged) static pressure, psfa
$\tilde{p}$	Root-mean-square of fluctuating pressure, psf
$\tilde{p}_a$	Root-mean-square of fluctuating acoustic pressure, psf
$\tilde{p}_v$	Root-mean-square of vorticity-induced pressure fluctuation, psf
q_∞	Free-stream dynamic pressure, psf
R_D	Disturbance Reynolds number (Eq. 1)
R_{DC}	Critical value of disturbance Reynolds number
R_E	Unit Reynolds number, 1/ft
$R_E X_t$	Transition Reynolds number
T_W	Transition body wall temperature, °R
T_∞	Free-stream static temperature, °R

$\tilde{u}$	Root-mean-square of fluctuating velocity, ft/sec
u_∞	Free-stream velocity, ft/sec
X_{rms}	Distance to maximum value of the root-mean-square of the axial pitot pressure traverse, Fig. 3
X_T	Distance to end of transition as defined by the peak in the axial pitot probe pressure traverse, Fig. 3
X_t	Distance to beginning of transition as defined by the rise in the axial pitot probe pressure traverse, Fig. 3
x	Axial distance, in.
y	Transverse boundary-layer coordinate, ft
Z	Boundary-layer acoustic impedance
ΔC_p	Dynamic pressure coefficient, p/q_∞
δ	Boundary-layer thickness, ft
η	Nondimensional transverse boundary-layer coordinate, y/δ
η_c	Transverse distance to critical value of disturbance Reynolds number
Λ	Pohlhausen shape factor for compressible flow
λ_a	Acoustic disturbance scale length
λ_v	Vorticity scale length
μ	Laminar viscosity, ft^2/sec
ν_∞	Kinematic viscosity based on free-stream density, ft^2/sec
ρ_w	Fluid density at transition body surface, lbm/ft^3
ρ_∞	Free-stream static density, lbm/ft^3
Σ	Disturbance parameter, see Eq. (6a)
τ	Tunnel wall porosity
χ	Scale length for mean pressure gradient

CONTENTS

ILLUSTRATIONS

NOMENCLATURE

A   Value of $F'(\eta)$ at η_c

a_∞ Free-stream speed of sound, ft/sec

B   Value of $G'(\eta)$ at η_c

C   Constant of proportionality between boundary-layer thickness and Reynolds number

F(y), G(y)   Polynomial functions of y in Pohlhausen boundary-layer velocity profile

f   Compressibility correction factor

K_1 Constant defined in Section 3.1

K_2 Constant defined in Section 3.1

k R_D/C

k_1 $k\sqrt{R_E X_t}$

L   Prandtl mixing length

ℓ Characteristic length of transition model, 36 in.

M   Mach number

M_f Fluctuating Mach number based on root-mean-square fluctuating velocity component

p   Pressure, psfa

$\bar{p}$ Steady-state (time-averaged) static pressure, psfa

$\tilde{p}$ Root-mean-square of fluctuating pressure, psf

$\tilde{p}_a$ Root-mean-square of fluctuating acoustic pressure, psf

$\tilde{p}_v$ Root-mean-square of vorticity-induced pressure fluctuation, psf

q_∞ Free-stream dynamic pressure, psf

R_D Disturbance Reynolds number (Eq. 1)

R_{DC} Critical value of disturbance Reynolds number

R_E Unit Reynolds number, 1/ft

$R_E X_t$ Transition Reynolds number

T_W Transition body wall temperature, °R

T_∞ Free-stream static temperature, °R

$\tilde{u}$	Root-mean-square of fluctuating velocity, ft/sec
u_∞	Free-stream velocity, ft/sec
X_{rms}	Distance to maximum value of the root-mean-square of the axial pitot pressure traverse, Fig. 3
X_T	Distance to end of transition as defined by the peak in the axial pitot probe pressure traverse, Fig. 3
X_t	Distance to beginning of transition as defined by the rise in the axial pitot probe pressure traverse, Fig. 3
x	Axial distance, in.
y	Transverse boundary-layer coordinate, ft
Z	Boundary-layer acoustic impedance
ΔC_p	Dynamic pressure coefficient, p/q_∞
δ	Boundary-layer thickness, ft
η	Nondimensional transverse boundary-layer coordinate, y/δ
η_c	Transverse distance to critical value of disturbance Reynolds number
Λ	Pohlhausen shape factor for compressible flow
λ_a	Acoustic disturbance scale length
λ_v	Vorticity scale length
μ	Laminar viscosity, ft^2/sec
ν_∞	Kinematic viscosity based on free-stream density, ft^2/sec
ρ_w	Fluid density at transition body surface, lbm/ft^3
ρ_∞	Free-stream static density, lbm/ft^3
Σ	Disturbance parameter, see Eq. (6a)
τ	Tunnel wall porosity
χ	Scale length for mean pressure gradient

SECTION I
INTRODUCTION

A criterion for the onset of laminar breakdown to turbulent flow has been the goal of gasdynamists for many years. It was Reynolds who first suggested that this transition was initiated by an instability in the laminar flow. Since that time stability analysis has been repeatably applied to the problem. Lord Rayliegh used a linear inviscid analysis to establish the basic stability criteria for a laminar flow (Ref. 1). Later, Tollmien and Schlichting (Ref. 1) used stability theory to predict the growth of an infinitesimal disturbance in a boundary layer on a flat plate. Their analysis showed that above a certain critical Reynolds number such disturbances would grow. They suggested that once these instabilities grew sufficiently large, they induced transition. The experiments of Schubauer and Skramstad (Ref. 2) verified the presence of linear waves in the boundary layer on a flat plate. In the course of their investigation, they demonstrated that the free-stream disturbance levels affected the transition location. They speculated that at their lowest values of the free-stream turbulence intensity (i.e., $\tilde{u}/u_\infty$), the velocity fluctuations were significantly influenced by the acoustic environment established by their test facility. Recently, Wells (Ref. 3) obtained transition data in an ultraquiet flow facility in which the acoustic levels were an order of magnitude lower than the acoustic level of Ref. 2. Wells obtained a zero disturbance level value of approximately 5×10^6 for the transition Reynolds number as compared to 2.8×10^6 obtained by Schubauer and Skramstad.

Because the linear theory and its nonlinear progeny have not been able to locate transition explicitly, the exact transition mechanism remains in doubt. However, it has been suggested for some time, although not experimentally demonstrated, that breakdown is initiated when the ratio of the inertial shearing stresses to the laminar viscous shearing stresses reaches some critical value. Liepmann (Ref. 4) first suggested that this ratio becomes a maximum somewhere in the boundary layer near the "critical layer" of the stability theory. On this assumption, he developed an expression to predict transition location which depended upon the linear stability theory amplification factor, the unit Reynolds number, and the initial magnitude of the free-stream velocity fluctuations. His method gave moderately good results (Ref. 5). Since then, there have been several prediction techniques that use either the linear stability theory, Liepmann's hypothesis, or both. Many have had moderately good agreement with experimental data (Ref. 6).

J.W. Elder obtained a good insight into the basic mechanisms which induce transition (Ref. 7). His experiments on a flat plate showed that there exists a critical ratio of the local fluctuating velocity component to the local mean velocity prior to turbulent spot formation in the boundary layer. This result lends support to the formulation of van Driest and Blumer (Ref. 8), who postulated that the ratio of the inertial to laminar shearing stresses reaches a critical value (which is a constant) prior to laminar breakdown. Their final result is an expression involving the transition Reynolds number and the magnitude of the free-stream velocity fluctuations only.

1

The effect of free-stream disturbances is not restricted to the low subsonic speed range as the references quoted above may imply. Boltz, et al. (Ref. 9) investigated several geometries from the low-speed range to the high subsonic. They found that test facility acoustic levels affected transition location. Pate and Schueler (Ref. 10) and Pate (Ref. 11) have shown that supersonic and hypersonic transition locations are dependent on acoustic radiation from test section wall turbulent boundary layers. They have developed a correlation involving only acoustic parameters and tunnel size to predict the transition Reynolds number on a 10-deg included-angle cone and a flat plate for these flow regimes. Other extensive work at the Arnold Engineering Development Center (AEDC) by Credle (Ref. 12), Credle and Carleton (Ref. 13), and Credle and Shadow (Ref. 14) using a 10-deg included-angle cone has also demonstrated the influence of free-stream acoustic disturbances in the transonic flow regime.

SECTION II
ANALYSIS

2.1 THE DISTURBANCES

Before proceeding to the development of the model, it would be well to consider the characteristics of the disturbances encountered in wind tunnel testing that influence boundary-layer transition. Schubauer and Skramstad found that the disturbance level in their tunnel increased with increasing free-stream velocity (Ref. 2). Pate and Schueler showed that the noise radiated from the turbulent boundary layer on the test section wall decreased with increasing Reynolds number for a fixed supersonic Mach number (Ref. 10). The transonic flow regime has proven to be considerably more complex. The investigations of Refs. 12, 13, and 14 have determined that there is no clear-cut dependence of the disturbance level on flow variables (i.e. Mach number, Reynolds number, etc.) but rather, that the disturbance level depends very much upon test section wall and tunnel configurations. The general level of acoustic radiation found in a perforated wall transonic tunnel is shown in Fig. 1.

One feature is common to all the above studies, regardless of the flow regime: when the magnitude of the disturbances increases for fixed flow conditions, boundary-layer transition moves forward. Since the magnitude of the disturbance varies from one facility to another, the observed variation in the transition data taken on the same model but in different flow facilities (Refs. 10 through 14) was not totally unexpected. Therefore, the possibility still exists that all of the transition data described above may be correlated by a single technique if the interaction between the free-stream disturbances and the model boundary layer is properly understood.

2.2 ANALYTICAL DEVELOPMENT

The experimental findings of Elder (Ref. 7) and the success of van Driest and Blumer (Ref. 8) indicate that the assumption of a critical ratio of inertial stress to viscous stress for laminar breakdown is valid, at least to a first approximation. Such an assumption
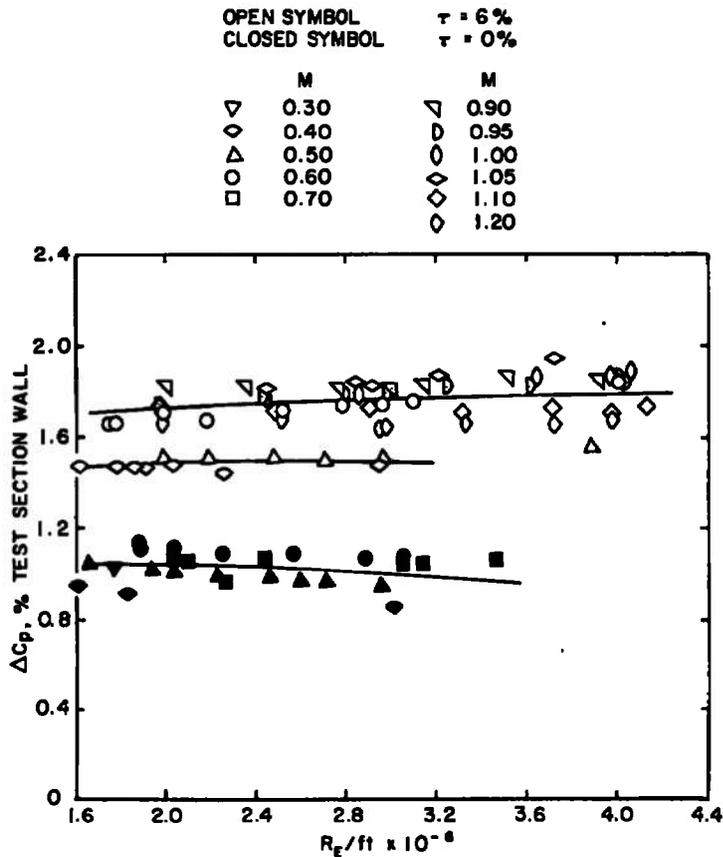
Fig. 1 Variation of Transonic Acoustic Levels with Unit Reynolds Number (Tunnel 4T)

has the additional feature of being applicable regardless of flow regime. As developed in Refs. 4 and 8, the shear stress ratio can be written in terms of a disturbance Reynolds number, R_D, as

$$R_D = \rho \overline{u_i u_j} / (\mu \partial u / \partial y) \tag{1}$$

where $\rho \overline{u_i u_j}$ is the Reynolds (or inertial) stress and $\mu \partial u / \partial y$ is the laminar shear stress. The critical value of R_D, R_{D_C}, is assumed to attain the same constant value at breakdown to turbulence. This critical value can be expected to occur in the interior of the boundary layer near the "critical layer" of stability theory, which is in the neighborhood of the maximum critical velocity ratio measured by Elder. Since Eq. (1) is not particularly convenient for estimating the location of transition, it may be put in a more suitable form by eliminating the inertial stresses in terms of a suitable correlation with the mean flow. This is done by employing the Prandtl mixing-length hypothysis and the Pohlhausen velocity profile. Letting the Prandtl mixing length be L, the inertial stress can be expressed as

$$\rho \overline{u_i u_j} = \rho L^2 (\partial u / \partial y)^2 \tag{2}$$

3

The velocity profile can be written in terms of the nondimensional distance $\eta = y/\delta$ as

$$u/u_\infty = F(y) + \Lambda G(y) \qquad (3)$$

where F and G are polynominals in η, Λ is $(\rho_\infty/\rho_w)(\delta^2/\nu_\infty\rho_\infty u_\infty)\,\partial p/\partial x$, the Pohlhausen shape factor, and the subscript ∞ denotes conditions at the boundary-layer edge. Equation (1) may be rewritten in terms of Eqs. (2) and (3) as

$$R_D = R_E(L^2/\delta)[F'(\eta) + \Lambda G'(\eta)] \qquad (4)$$

where F' and G' are the derivatives of F and G with respect to η and R_E is the unit Reynolds number in appropriate units.

The effects of the free-stream disturbances can now be entered into the formulation through the pressure gradient term. It is assumed that the instantaneous pressure, p, is composed of a mean and a fluctuating part, $\overline{p}$ and $\widetilde{p}$, respectively. It is further assumed that the fluctuating pressure can be expressed as a linear combination of two terms: one caused by acoustic disturbances and one caused by vorticity disturbances. This separation is expected to be a reasonable approximation up to the low supersonic flow regime (M < 2.0) at least, and for moderate levels of the pressure field. The shape factor, which accounts for the effects of pressure gradients, can now be written as

$$\Lambda = \frac{\rho_\infty}{\rho_w}\frac{\delta^2}{\nu_\infty\rho_\infty u_\infty}\left(\frac{\partial\overline{p}}{\partial x} + \frac{\partial\widetilde{p}_v}{\partial x}f + \frac{\partial\widetilde{p}_a}{\partial x}Z\right)$$

where the coefficient f is a compressibility correction factor and is given by Hinze (Ref. 15) as $(1 + \beta M^5{}_f)^{1/2}$ where $\beta = 40$ and $M_f = \widetilde{u}/a_\infty$. Since $\widetilde{u}/u_\infty$ is less than 3 percent in most wind tunnels, the above correction is small, and f will be taken to be equal to 1. The coefficient Z is the boundary-layer acoustic impedance.

A further approximation is made on the two fluctuating pressure gradients: $\partial\widetilde{p}_v/\partial x \sim \widetilde{p}_v/\lambda_v$ and $\partial\widetilde{p}_a/\partial x \sim \widetilde{p}_a/\lambda_a$ where λ_v and λ_a are appropriate scale lengths. No such approximation can be made on the mean pressure gradient because the appropriate scale length, χ, depends upon actual flow conditions. However, as long as the boundary-layer approximations hold, it can be expected that the mean gradient will be negligible over the scale of the disturbances. The shape factor is

$$\Lambda = \frac{\rho_\infty}{\rho_w}\frac{\delta^2}{\nu_\infty\rho_\infty u_\infty}\left(\frac{1}{\chi}\frac{\partial\overline{p}}{\partial x} + \frac{\widetilde{p}_v}{\lambda_v}f + \frac{\widetilde{p}_a}{\lambda_a}Z\right)$$

A final approximation can be made to the fluctuating pressures since the acoustic variations are primarily linear pressure fluctuations and the vorticity variations are primarily velocity fluctuations (Ref. 16). Taylor (Ref. 17) showed that the latter are related to

the corresponding pressure variations by $\tilde{p}_v \cong \rho \tilde{u}^2$ where $\tilde{u}$ is the root-mean-square (rms) velocity fluctuation. Incorporating these approximations into the previous expression for the shape factor gives

$$\Lambda = \frac{\rho_\infty}{\rho_w} \frac{\delta^2}{\nu_\infty \rho_\infty u_\infty} \left(\frac{1}{X} \frac{\partial \overline{p}}{\partial x} + \frac{\rho \tilde{u}^2}{\lambda_v} + \frac{\tilde{p}_a}{\lambda_a} Z \right) \tag{5}$$

Substiting Eq. (5) into Eq. (4) and evaluating the result at the point in the boundary layer where the critical value of R_D occurs ($\eta = \eta_c$) yields

$$R_{D_C} = R_E \frac{L^2}{\delta} \left(A + B \frac{T_W}{T_\infty} R_E \frac{\delta^2}{\lambda_v} \Sigma \right) \tag{6}$$

where the constants A and B are the values of $F'(\eta)$ and $G'(\eta)$ evaluated at $\eta = \eta_c$. The function Σ is defined as

$$\Sigma = \frac{\lambda_v}{2q_\infty} \frac{1}{X} \frac{\partial \overline{p}}{\partial x} + \frac{Z}{2} \frac{\lambda_v}{\lambda_a} \Delta C_p + \left(\frac{\tilde{u}}{u_\infty} \right)^2$$

where q_∞ is the dynamic pressure in the free stream and $\Delta C_p = \tilde{p}_a/q_\infty$. The function Σ gives a mechanism whereby the free-stream disturbances contribute to the ratio of the Reynolds-to-laminar shearing stresses.

To apply Eq. (6) to a flow where the disturbance magnitudes are known, it is necessary to estimate the length scales. According to Ref. 8, the appropriate lengths are δ for L and 0.6δ for λ_v. If the boundary-layer thickness, δ, is assumed to vary as

$$\delta \simeq C x^{\frac{1}{2}} / R_E^{\frac{1}{2}}$$

then Eq. (6), which is the value of R_D where transition begins, can be rewritten to obtain

$$R_{D_C} = C\sqrt{R_E X_t} (1 + 0.1 C T_W/T_\infty \sqrt{R_E X_t} \Sigma) \tag{7}$$

where $R_E X_t$ is the beginning of transition Reynolds number based on appropriate distance (e.g., the distance from the cone vertex). The constants A = 1.10 and B = 0.1 are approximated by evaluating them at $\eta_c = 0.5$ (Ref. 8 gives $\eta \approx 0.6$).

The behavior of $R_E X_t$ as the external disturbances vanish (i.e., $\Sigma \to 0$) can be obtained from Eq. (7) as

$$\lim_{\Sigma \to 0} R_{D_C} = \lim_{\Sigma \to 0} [C\sqrt{R_E X_t}(1 + 0.1 C T_W/T_\infty \sqrt{R_E X_t} \Sigma)]$$

$$= C\sqrt{R_E X_t} = \text{constant, by assumption}$$

which implies that the transition Reynolds number, $R_E X_t$, for zero disturbances is a constant.

Equation (7) can be rearranged slightly by dividing through by the quantity in brackets. Then, if $0.1 C (T_W/T_\infty)\sqrt{R_E X_t}\ \Sigma < 1$, use of the binominal theorem leads to

$$\sqrt{R_E X_t} = k[1 - 0.01\ CT_W/T_\infty \sqrt{R_E X_t}\Sigma + O(\Sigma^2)] \qquad (8)$$

where $k = R_D/C$. This gives a correction to the transition Reynolds number for small values of the free-stream disturbances.

2.3 VALUES OF THE CONSTANTS

Equation (8) will be suitable for calculation of the transition Reynolds number if all the values of the constants are specified. An estimate of the ratio of λ_v/λ_a can be obtained by considering that those wavelengths that can most effectively disrupt the boundary layer are those which impress a shear on the entire layer. This condition would imply that $\lambda_a \gg \delta$. Therefore, it can be expected that $\lambda_v/\lambda_a \ll 1.0$. For convenience in the calculations, $\lambda_v/\lambda_a = 0.1$ will be taken. The value $\overline{\lambda_v/\chi} \ll 1$ is taken as being appropriate to the 10-deg cone. Since the boundary-layer interaction with the incoming disturbances is not well known, the boundary-layer impedance, Z, will be taken as 1. Finally, the boundary-layer thickness proportionality constant, C, is given for a flat plate in Ref. 1 as C = 5. Correcting this value for axisymmetric flow gives C = 1.67.

The remaining constant can be estimated by evaluating Eq. (8) for available transition data. However, it is somewhat easier to evaluate Eq. (8) if the square roots are first removed by squaring both sides. Then, for sufficiently small values of Σ, $R_E X_t$ is approximately constant so that, to the first order,

$$R_E X_t = k(1 - k k_1 T_w/T_\infty \Sigma) \quad , \qquad k_1 = k\sqrt{R_E X_t}$$

As a check, the mean pressure gradient for a 10-deg included-angle cone was calculated and found to be negligible compared to the measured values of ΔC_p. Further, unpublished measurements of the fluctuating velocities in the Propulsion Wind Tunnel Facility (PWT) Propulsion Wind Tunnel (16T) and Aerodynamic Wind Tunnel (4T) were found to be of the order expected for the measured values of the acoustic disturbances. To illustrate this point briefly, the measured values of $\widetilde{u}/u_\infty$ were found to be approximately from 0.01 to 0.02. The measured fluctuating pressure levels (ΔC_p) were also found to be approximately from 0.01 to 0.02. If the pressure fluctuation is assumed to be caused completely by vorticity, then the corresponding pressure levels should vary as the square root of the measured velocity variation; i.e., $\widetilde{p}_{measured} \sim (\widetilde{u}/u_\infty)^2$. On the other hand, the pressure fluctuations should vary linearly with the oscillation velocity if they are completely acoustic in nature (Ref. 16). Since the measured velocity oscillations are of the same order as the measured pressure fluctuations, it is assumed that the pressure

oscillations produced by vorticity in the free stream are negligible compared to the acoustic pressure oscillations. Therefore, $(\tilde{u}/u_\infty)^2 \ll \Delta C_p$ was taken as an additional approximation.

Figure 2 shows the variation of $R_E X_t$ as a function of $(T_W T_\infty)\Sigma$. It should be noted that the beginning of transition used throughout this paper was defined similarly to that of Ref. 2 (i.e., as the axial position where the pitot pressure begins to rise toward a peak). The various locations are illustrated in Fig. 3. The beginning of the rise was used rather than the peak of the pressure curve, as in Refs. 10 and 11, because it is closer to the point of laminar breakdown. The value of $R_E X_t$ at $\Sigma = 0$ from Fig. 2 was taken to be $R_E X_t = 3 \times 10^6$.
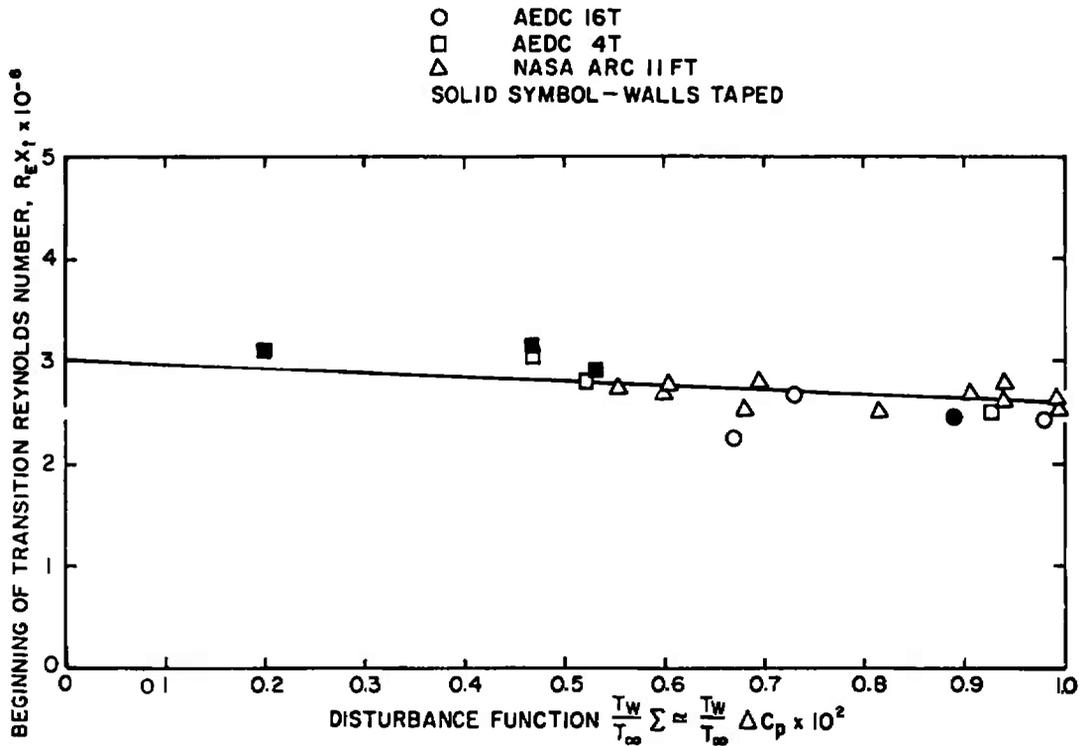
Fig. 2 Transition Reynolds Number Variation with Disturbance Function

This zero disturbance value can be used to obtain the value of $R_{DC} = 2890$ from Eq. (8). Van Driest and Blumer (Ref. 8) obtained a value of 1690 based on the flat-plate data of Schubauer and Skramstad (Ref. 2), and Wells (Ref. 3) obtained a value of 2220 in a considerably quieter test facility. These two values used for comparison are for low subsonic flows over flat plates. The agreement is reasonable, although not exact, and tends to lend qualitative support to the critical disturbance Reynolds number assumption.
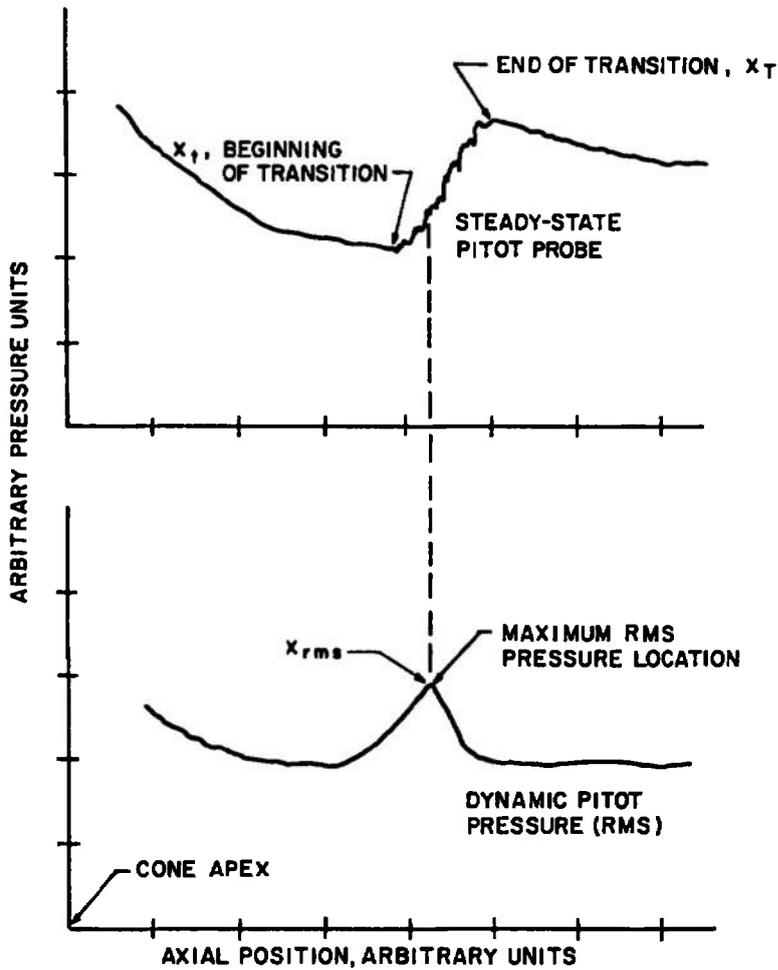
Fig. 3 Typical Pitot Traverses and Definition of Transition Locations

SECTION III
COMPARISON WITH EXPERIMENT

3.1 FINAL ANALYTICAL EXPRESSION

The most accurate test of the adequacy of the analytical procedure would be a direct comparison of predicted transition location to the measured value for given flow conditions. To this end, Eq. (8) was rearranged in the form

$$\left(\frac{X_t}{\ell}\right)^2 - \left[\frac{2K_1}{R_E} + \left(\frac{K_1 K_2}{\sqrt{R_E}} \frac{T_W}{T_\infty} \Sigma\right)^2\right]\left(\frac{X_t}{\ell}\right) + \left(\frac{K_1}{R_E}\right)^2 = 0 \qquad (9)$$

where terms of order Σ^2 and higher have been neglected compared to unity. The values of the constants given in Section 2.3 were altered so that ΔC_p and $(\tilde{u}/u_\infty)$ could be entered in percent, and R_E could be entered in millions. Equation (9) was then solved using as values of the constants, $\ell = 3.0$ ft, $K_1 = 1.0$, and $K_2 = 0.0577$.

3.2 COMPARISONS IN THE TRANSONIC FLOW REGIME

A considerable quantity of transition data on a 3-ft, 10-deg included-angle cone has been accumulated by AEDC personnel. This includes extensive data from Tunnels 4T and 16T as well as from a number of other facilities throughout the United States. Therefore, a range of tunnel sizes, geometries, and test section relief techniques (i.e., slots, porous walls, etc.) was available for comparison.

Comparisons of the predicted transition location with the measured locations are shown in Fig. 4. The rms acoustic measurements used in the calculations were taken from one of two cone-mounted microphones located 18 and 26 in. behind the cone apex. It was assumed that these measurements were representative of the acoustic environment of the cone. (See Ref. 18 for a more detailed discussion of this point.) Primarily, the data from the forward microphone were used in the prediction technique; when transition occurred over the forward microphone, the aft measurements were used.
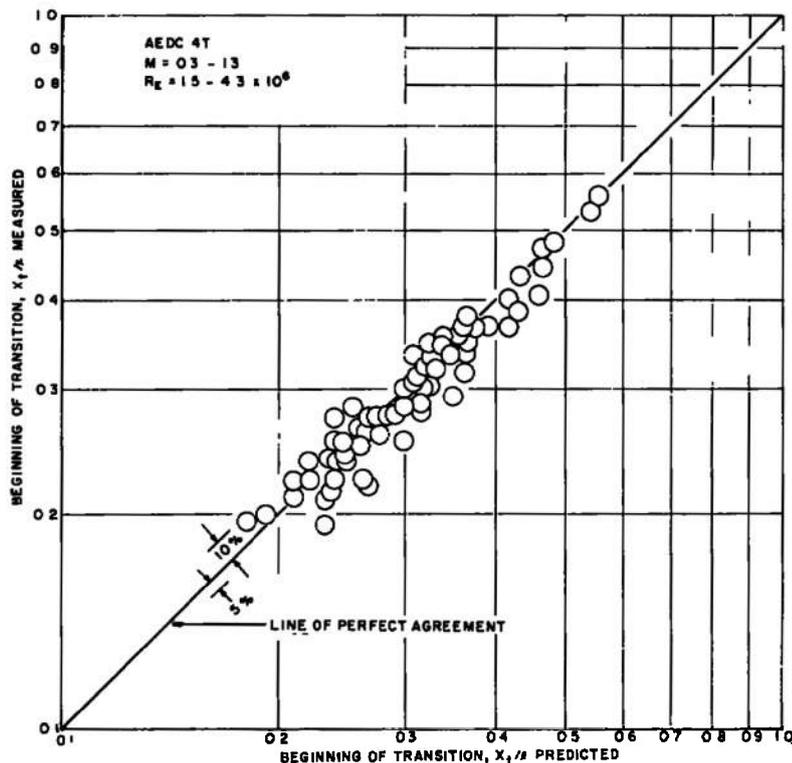
a. Tunnel 4T
Fig. 4 Comparison of Predicted and Measured Transition Locations
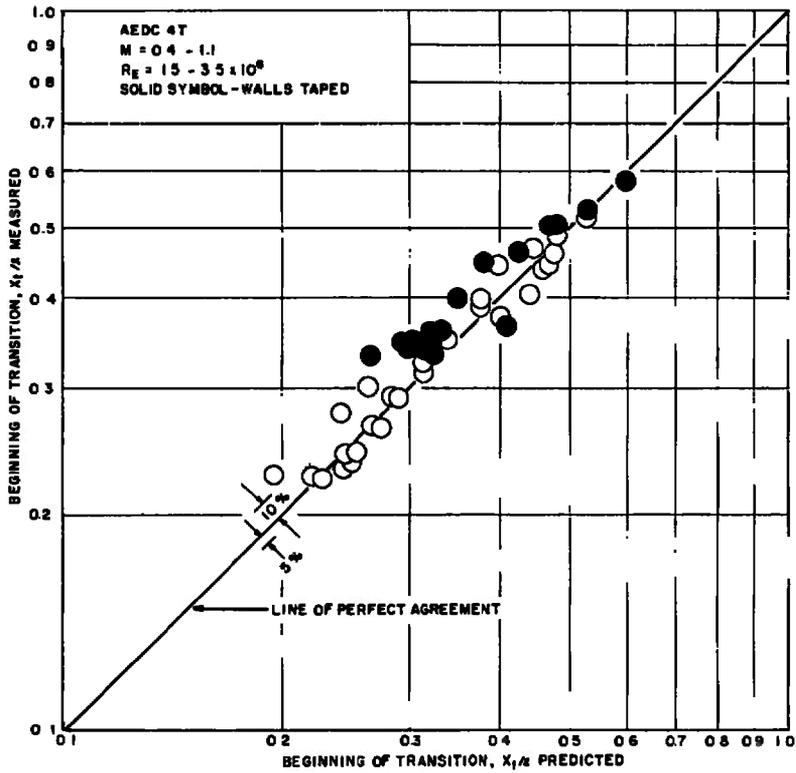
b. Tunnel 4T, Continued
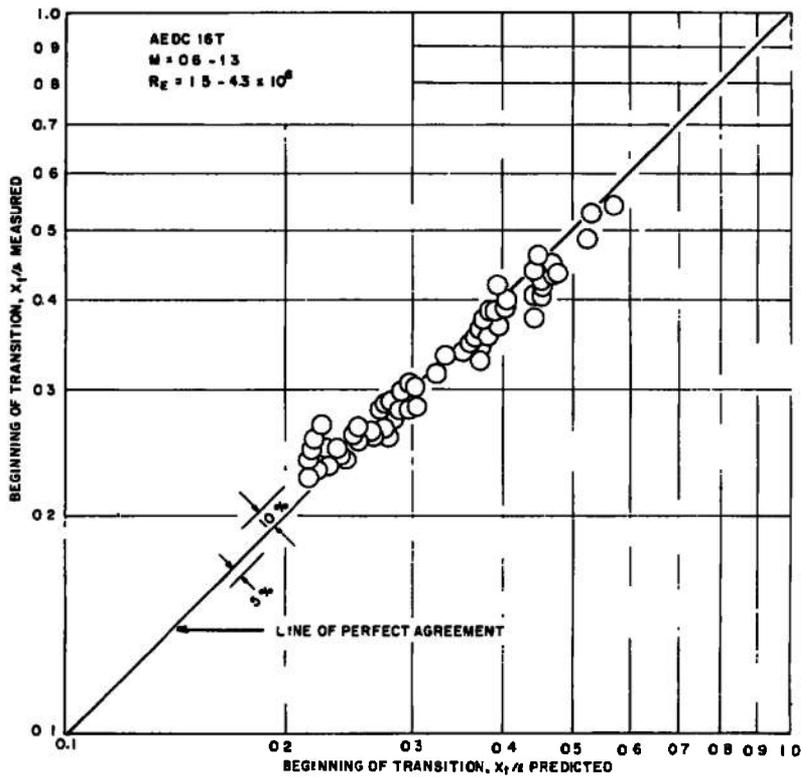
c. Tunnel 16T

Fig. 4 Continued
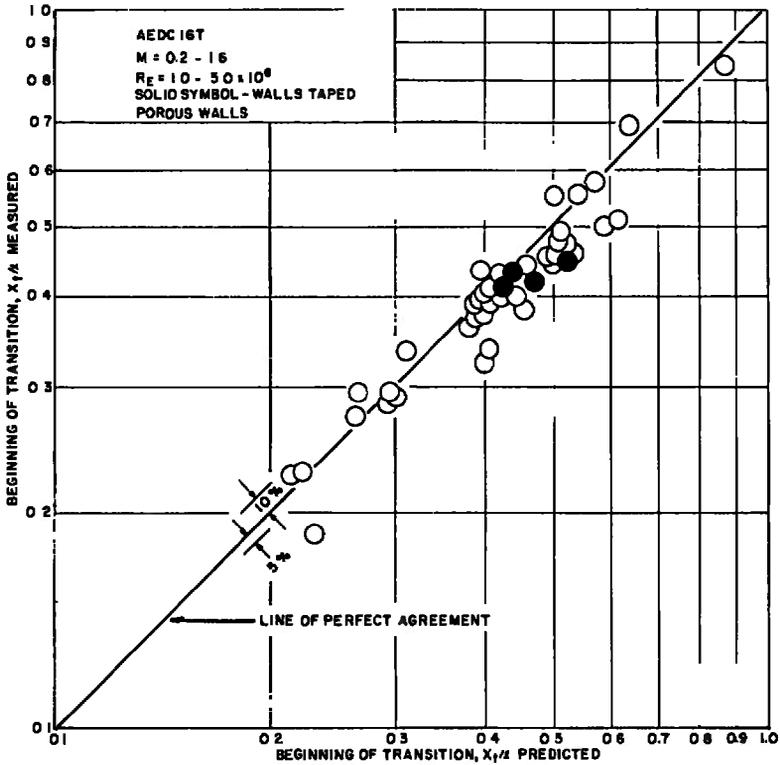
d. Tunnel 16T, Continued
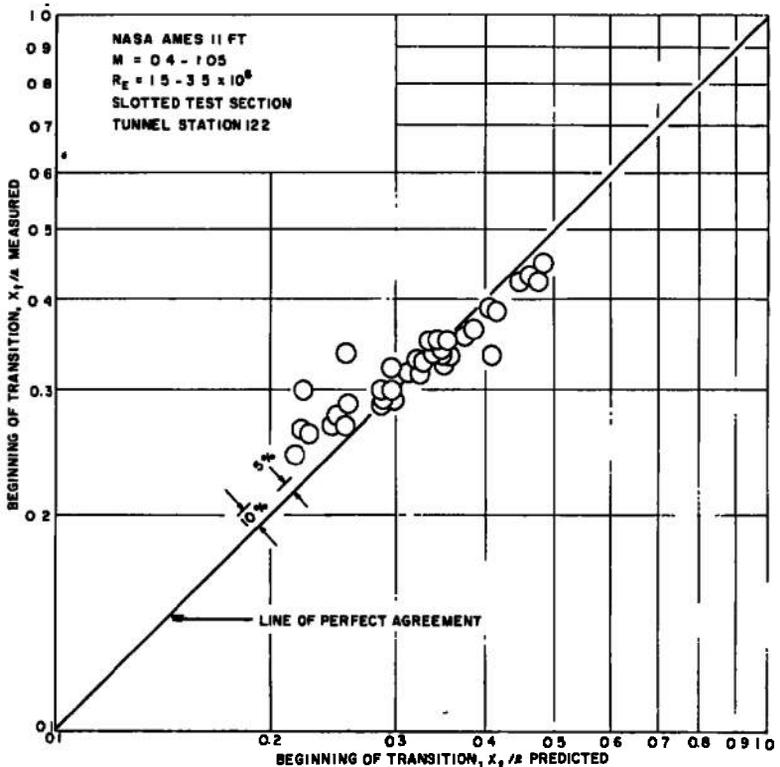
e. NASA Ames 11-ft Tunnel (Station 122)

Fig. 4 Continued
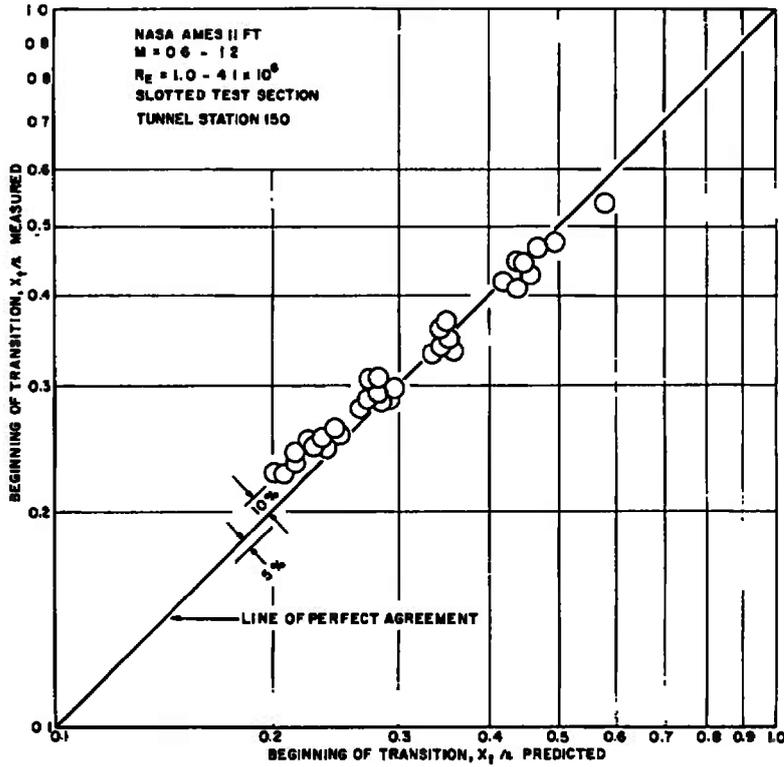
f. NASA Ames 11-ft Tunnel (Station 150)
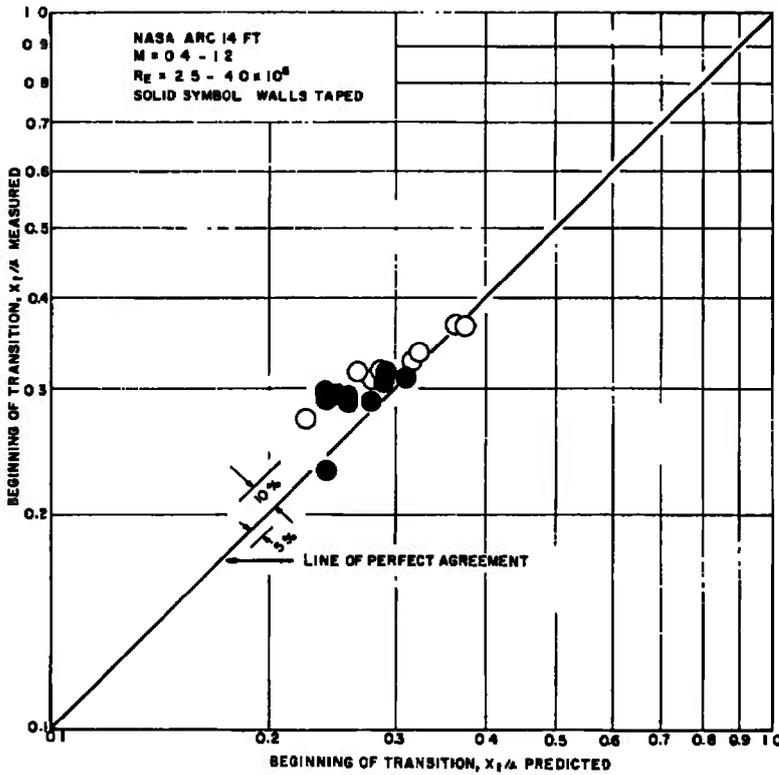
g. NASA Ames 14-ft Tunnel
Fig. 4 Concluded

12

3.3 DISCUSSION OF THE RESULTS

Figure 4 indicates that 60 to 70 percent of the transition data can be predicted to within 5 percent with reasonable consistency and that 90 percent of the data can be predicted within 10 percent. Some of the error is attributable to the uncertainty of locating the transition point from the data. It was found that there was approximately a 3-percent maximum variation between the values of X_t obtained by independent reduction of the same data. Therefore, the error band observed in the figure can be only partially ascribed to the data reduction process. Some of the data from Tunnel 4T (Fig. 4a) were obtained with simultaneous velocity fluctuation (hot-wire probe) and noise level (microphone) measurements. It was found that the hot-wire probe influenced the cone transition measurements under some conditions.

It is believed that another source of error is the variation of the cone angle of attack under dynamic loading. The effect of pitch misalignment at two Mach numbers is illustrated in Fig. 5. As indicated, misalignment of only one degree can easily induce a variation of as much as 10 percent in transition location. Although the cone was installed with great care to assure its initial alignment, measurements were not made of the cone deflections under dynamic loading. Therefore, such effects cannot be removed from the data.
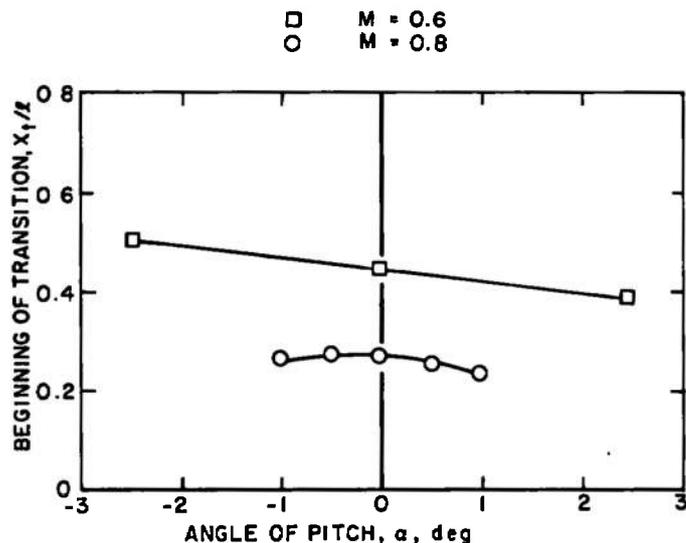
Fig. 5 Variation of Transition Location with Angle of Attack

An additional factor which could influence the agreement between the predicted and observed transition is the effect of the cone boundary layer on the free-stream disturbances passing through it. This aspect is further complicated by the observation that the location

of transition relative to the microphone location influences the noise level observed. Figure 6 illustrates the effect of unit Reynolds number on cone acoustic measurements for two test section configurations of Tunnel 4T at several Mach numbers. The data peaks observed are caused by the passage of transition over the microphone location as the Reynolds number is decreased. The figure indicates that the perforated wall (open symbols) data were obtained at higher acoustic disturbance levels, and evidence of peaking of the pressure fluctuations is postponed until lower unit Reynolds numbers.
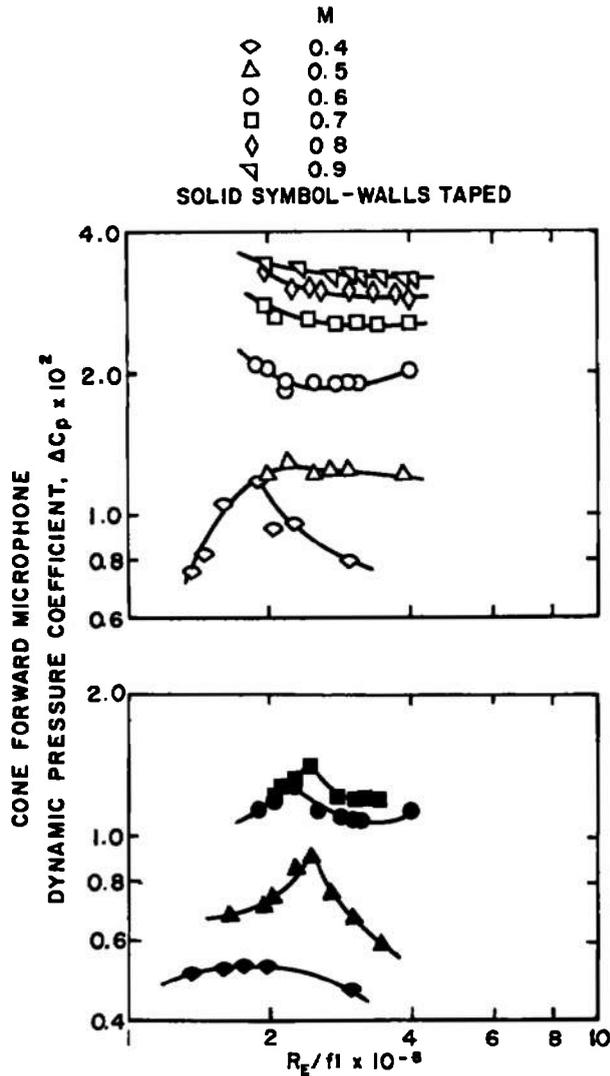
Fig. 6 Dynamic Pressure Coefficient Variations with Unit Reynolds Number

Figure 7 gives the variation of the intensity $(\tilde{p}^2/\rho_\infty a_\infty \Rightarrow \tilde{p}/\rho_t M^3)$ of the acoustic disturbances with measured end of transition location. Mr. O. P. Credle has determined from the pitot probe data that the ratio of the distance to the rms peak (Fig. 3), X_{rms}, to the distance to the end of transition, X_T, is constant explicitly, $X_T/X_{rms} \cong 1.11$. Thus, the maximum rms location noted on the figure is the location where end of transition must occur for the rms peak to be over the microphone. Therefore, it would appear that the passage of the rms peak caused the peaks observed in Fig. 6. Further, the acoustic intensity at the cone appears to be constant for constant Mach number when transition does not occur near the microphone. Finally, the difference between the forward and aft microphone measurements is illustrative of the cone boundary-layer effects on the measured acoustic levels. Unfortunately, there is no method available at present that allows corrections to the available acoustic data for these effects.
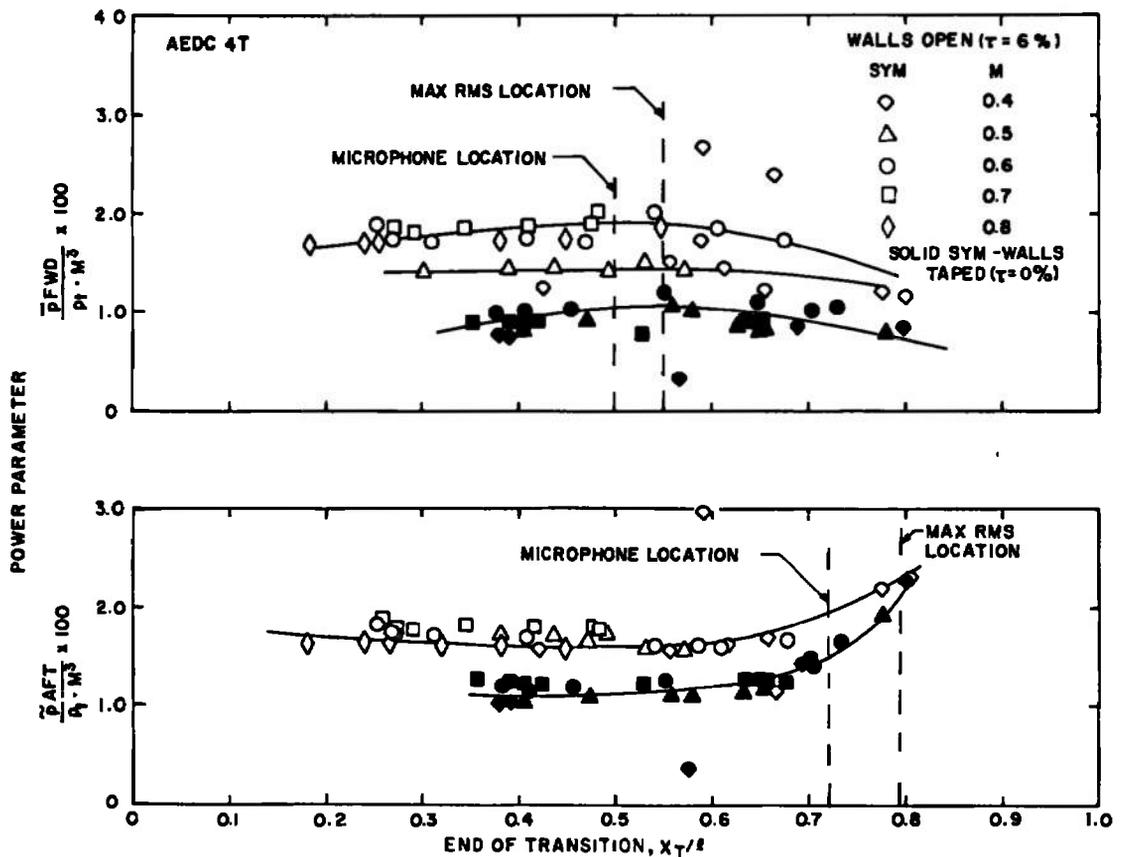
Fig. 7 Acoustic Intensity Measurement at Two Cone Locations as a Function of End of Transition Location

3.4 COMPARISONS IN OTHER FLOW REGIMES

In order to determine the extent of the applicability of the present analysis, comparisons were made with available data in the supersonic and low-speed flow regimes. The 4-ft long, 10-deg included-angle cone data of Pate (Ref. 11) were used for the supersonic comparison. Since Pate had measured the end of transition, as defined here, it was necessary to take the beginning of transition from axial pitot traverses presented in Ref. 11. A large quantity of this type of data was, understandably, not available; therefore, the extent of the comparison is not extensive. The noise data for Tunnel A was taken from Ref. 10, where ΔC_p is given as a function of unit Reynolds number per inch for Mach numbers 3 and 5. The predicted and measured values of transition location are shown in Fig. 8. The data are predicted as accurately as the data from the transonic tunnels.
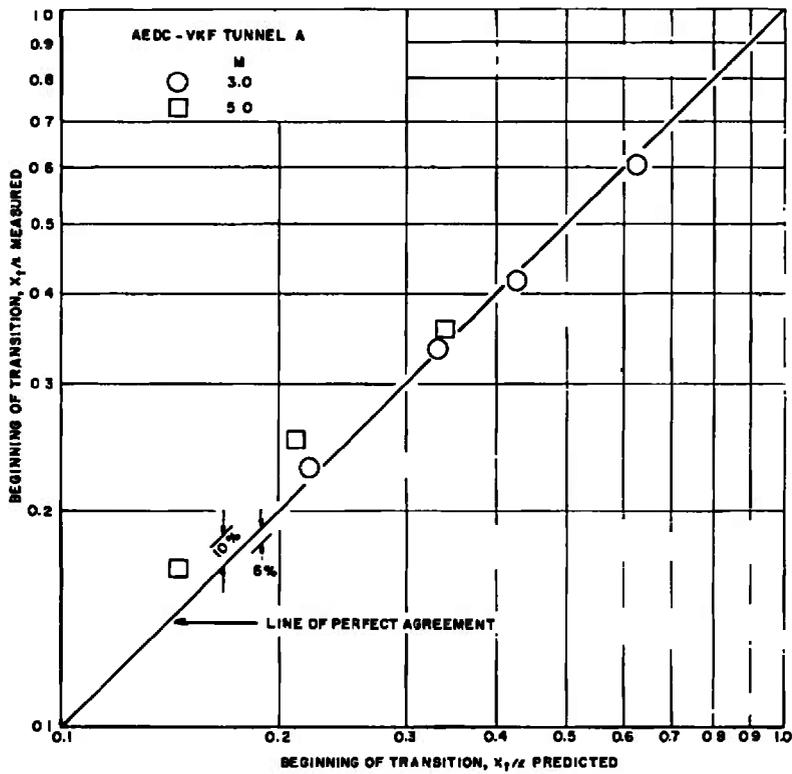
Fig. 8 Comparison of Predicted Supersonic Transition Location with the Measurements of Pate (Ref: 11)

The direct application of the correlation to low-speed transition data was hindered by the lack of measurements of the associated acoustic levels. The data of Refs. 2 and 3 were considered in detail, and the data of Schubauer and Skramstad (Ref. 2) were found to be the most similar to the previous data. The reason for this is that the noise

16

levels quoted by the authors of Ref. 2 were in the 105- to 110-db range, which corresponds to the lowest acoustic levels in the previous transonic and supersonic comparisons. The transition number for zero disturbances in Ref. 2 was approximately 2.85 x 10^6, which is in good agreement with the value found from the transonic data. A calculation was made to predict acoustic levels from the correlation by determining the value of the disturbance function (Σ) required to give a specified transition Reynolds number. If one assumes that the vorticity level was given by the measured value of $\tilde{u}/u_\infty$, ΔC_p can be found from

$$\Delta C_p = \Sigma - \tilde{u}/u_\infty$$

and the fluctuating pressure rms level is

$$\tilde{p} = \Delta C_p \times q_\infty$$

The values calculated for the high and low transition Reynolds numbers (Ref. 2) based on u_∞ = 100 ft/sec ranged from 105 to 112 db.

However, such good agreement was not obtained with the data of Ref. 3, which has a zero disturbance transition Reynolds number of 4.9 x 10^6 with a noise level of 90 db. This noise level is an order of magnitude lower than that of Ref. 2. In a follow-up investigation by Spangler and Wells (Ref. 19), the transition process was found to depend strongly on the frequency spectrum of the free-stream disturbances rather than on amplitude for very low values of the disturbances. This effect would explain the inadequacy of the present technique to predict the low disturbance level transition data since frequency dependency is not accounted for in this method.

SECTION IV
CONCLUSIONS

The previous section gave a comparison of predicted and measured boundary-layer transition locations and a brief discussion of the primary factors affecting the data. In view of the consistency of the results described, it may be concluded that the present analytical technique is justified, at least for 10-deg included-angle cones. However, it is desirable to apply these criteria to other geometries to assess their true value as a transition prediction scheme. Future efforts will be made in this direction. Extensions of the present method may well await a more detailed modeling of the physical processes involved, which in turn may be dependent on more extensive experimental studies. Therefore, the present work is not presented as a final solution, but merely as a useful tool to be used in lieu of an exact analysis. With this in mind, the following conclusions are drawn from the present study:

1. The method of predicting transition location proposed in this paper consistently predicts measured values to within 10 percent in the transonic flow regime on 10-deg included-angle cones.

2. Initial comparisons with supersonic, and low subsonic data indicate that the method is extendible to these flow regimes.

3. Noise appears to be at least as important as vorticity in causing transition, and in many cases it is more important.

REFERENCES

1. Schlichting, H. Boundary-Layer Theory, translated by J. Kestin. McGraw-Hill Book Company, New York, 1960. (Fourth Edition).

2. Schubauer, G.B. and Skramstad, H.F. "Laminar-Boundary-Layer Oscillations and Transition on a Flat Plate." NACA Report 909 (1948).

3. Wells, C.S., Jr. "Effects of Free-Stream Turbulence on Boundary-Layer Transition." AIAA Journal, Vol. 5, No. 1, January 1967, pp. 172-174.

4. Liepmann, H.W. "Investigation of Boundary-Layer Transition on Concave Walls." NACA Report ACR 4J28, 1945.

5. Lin, C.C. The Theory of Hydrodynamic Stability. Cambridge University Press, New York, 1955.

6. Hairston, D.E. "Survey and Evaluation of Current Boundary Layer Transition Prediction Techniques." AIAA Paper 71-985, October 1971.

7. Elder, J.W. "An Experimental Investigation of Turbulent Spots and Breakdown to Turbulence." Journal of Fluid Mechanics, Vol. 9, Part 2, October 1960, pp. 235-246.

8. Van Driest, E.R. and Blumer, C.B. "Boundary-Layer Transition: Free-Stream Turbulence and Pressure Gradient Effects." AIAA Journal, Vol. 1, No. 6, June 1963, pp. 1303-1306.

9. Boltz, F.W., Kenyon, G.C., and Allen, C.Q. "The Boundary-Layer Transition Characteristics of Two Bodies of Revolution, a Flat Plate, and an Unswept Wing in a Low-Turbulence Wind Tunnel." NASA TN D-309, April 1960.

10. Pate, S.R. and Schueler, C.J. "Radiated Aerodynamic Noise Effects on Boundary-Layer Transition in Supersonic and Hypersonic Wind Tunnels." AIAA Journal, Vol. 7, No. 3, March 1969, pp. 450-457.

11. Pate, S.R. "Measurements and Correlations of Transition Reynolds Numbers on Sharp Slender Cones at High Speeds." AEDC-TR-69-172 (AD698326), December 1969.

12. Credle, O.P. "An Evaluation of the Fluctuating Airborne Environment in the AEDC-PWT 4-Ft Transonic Tunnel." AEDC-TR-69-236 (AD861673), November 1969.

13. Credle, O.P. and Carleton, W.E. "Determination of Transition Reynolds Numbers in the Transonic Mach Number Range." AEDC-TR-70-218 (AD875995), October 1970.

14. Credle, O.P. and Shadow, T.O. "Evaluation of the Overall Root-Mean-Square Fluctuating Pressure Levels in the AEDC PWT 16-Ft Transonic Tunnel." AEDC-TR-70-7 (AD864827), February 1970.

15. Hinze, J.O. Turbulence: An Introduction to Its Mechanism and Theory. McGraw-Hill Book Company, New York, 1959.

16. Morse, P.M. and Ingard, K.U. Theoretical Acoustics. McGraw Hill Book Company, New York, 1968.

17. Taylor, G.I. "Statistical Theory of Turbulence, Part V." Proceedings of the Royal Society of London, Vol. A156, 1936, pp. 307-317.

18. Pate, S.R. and Brown, M.D. "Acoustic Measurements in Supersonic Transitional Boundary Layers." AEDC-TR-69-182 (AD694071), October 1969.

19. Spangler, J.G. and Wells, C.S., Jr. "Effects of Free-Stream Disturbances on Boundary-Layer Transition." AIAA Journal, Vol. 6, No. 3, March 1968, pp. 543-545.

Security Classification

DOCUMENT CONTROL DATA - R & D

(Security classification of title, body of abstract and indexing annotation must be entered when the overall report is classified)

1 ORIGINATING ACTIVITY *(Corporate author)*	2a. REPORT SECURITY CLASSIFICATION
Arnold Engineering Development Center Arnold Air Force Station, Tennessee 37389	UNCLASSIFIED
	2b. GROUP N/A

3 REPORT TITLE

A METHOD FOR THE PREDICTION OF THE EFFECTS OF FREE-STREAM
DISTURBANCES ON BOUNDARY-LAYER TRANSITION

4 DESCRIPTIVE NOTES *(Type of report and inclusive dates)*
Final Report -- January 1972 through March 1973

5 AUTHOR(S) *(First name, middle initial, last name)*
J. A. Benek and M. D. High

6 REPORT DATE	7a. TOTAL NO OF PAGES	7b. NO OF REFS
October 1973	28	19

8a. CONTRACT OR GRANT NO.	9a. ORIGINATOR'S REPORT NUMBER(S)
b. PROJECT NO	AEDC-TR-73-158
c. Program Elements 64719F and 65802F	9b. OTHER REPORT NO(S) *(Any other numbers that may be assigned this report)*
d.	ARO-PWT-TR-73-88

10 DISTRIBUTION STATEMENT

Approved for public release; distribution unlimited.

11 SUPPLEMENTARY NOTES	12 SPONSORING MILITARY ACTIVITY
Available in DDC.	Arnold Engineering Development Center, Air Force Systems Command, Arnold AF Station, TN 37389

13. ABSTRACT

A semiempirical expression for boundary-layer transition location is developed based on the concept of a critical ratio of inertial to viscous shearing stresses at laminar breakdown. Extensive comparisons between predicted and measured transition locations on a 10-deg included-angle cone at transonic speeds are shown with the data predicted to within 10 percent. Comparisons are also made with low subsonic and supersonic data which indicate the method is extendible to these flow regimes.

DD FORM 1 NOV 66 **1473**

14 KEY WORDS	LINK A		LINK B		LINK C	
	ROLE	WT	ROLE	WT	ROLE	WT
boundary-layer separation						
laminar boundary layer						
turbulent flow						
aerodynamic noise						
transonic flow						

AFSC
Arnold AFS Tenn